

Safety Design of a Hybrid Wind-Solar Energy System for Rural Remote Areas in Costa Rica

Verónica Melissa Salas-Mora*, Gustavo Richmond-Navarro**

*Department of Architecture, Faculty of Engineering, Tokyo Polytechnic University, Kanagawa, Japan.

**Department of Electromechanical Engineering, Instituto Tecnológico de Costa Rica, 15 St, 14 Ave, Cartago, Costa Rica.

(vesamo003@gmail.com, grichmond@tec.ac.cr)

Corresponding Author; Verónica Melissa Salas-Mora, Washington State, United States, vesamo003@gmail.com

Received: 12.05.2019 Accepted: 01.09.2020

Abstract- Although several kinds of energy generation systems have been investigated and introduced in Costa Rica, none were made on systems that use more than one energy source. The present work proposes a safety design of a hybrid wind-solar renewable energy system, designed to cover the energy demand in a governmental free housing at Martina Bustos, Liberia, Costa Rica. Twelve scaled models were designed. These are composed by a pole and one to four solar panels. Two commercial wind turbines, Airdolphin Mark-Zero/Pro and Zephyr 9000 were used to experimentally measure wind force on a wind tunnel at the Wind Engineering Research Center of the Tokyo Polytechnic University. Further, allowable stress design was calculated to determine the tower resistance to local buckling. Present results indicate that towers with 200 mm of circumference and steel plates with 4.5 mm to 8 mm of thickness are considered safe from local buckling according to Japanese Industrial Standards. Energy generation calculation results show that four of the proposed models generate more than the average energy needed to supply electricity during a year at Martina Bustos to the specific house design.

Keywords- Hybrid renewable energy system; governmental free housing; wind tunnel; allowable stress design; local buckling.

1. Introduction

Electric energy is considered a basic service worldwide, however; many countries, still lack widespread access to electricity; despite rural electrification efforts [1]. Between 2011 and 2016, efficiency of electricity generation improved in all regions except Africa and Latin America. In these regions it decreased by 2.7% and 3.7%, respectively; and the global average efficiency of power generation increased from 41% to 43.1% [2]. In 2017, it was estimated that 73.5% of the energy share of global electricity production came from non-renewable sources [2]. However, most of the electricity produced comes from fossil fuels [1-2], which are precursors of global warming [3]. Thus, to ameliorate the negative impact countries and industries have developed strategies to generate electricity using alternative sources of energy, such as hydropower, wind and solar [4].

Hybrid renewable energy system (HRES) that use two or more limitless energy resources can be used to produce electricity for almost a year and contribute to the generation of clean energy by reducing greenhouse emissions at the same time, through an adequate system energy management [5]. This can be accomplished by changing the fuel power generation to a renewable off-grid micro power system [6] or stand-alone systems. These systems provide power to alternative current (AC) loads with a battery storage that has no connection to an external grid. Stand-alone systems performance can be improved through the implementation of adaptive controllers to optimize active power proportional integral (PI) parameters [7] or through algorithms of control. These algorithms are a result of the regulation of bidirectional converters between a battery and direct current (DC) bus [8] or a variety of applications. These systems can also be connected to a micro-grid [9], with capacitor banks in some

cases [10]. Although various renewable energy studies have been made globally, to supply electrification in single-family-houses for European countries [11], using high solar irradiation values and wind speeds between 5 m/s and 7 m/s in different islands [12], while evaluating economic and technical analysis of photovoltaic (PV)-wind-diesel hybrid systems in Arabic countries to generate energy [13], improving control of small wind turbines applications [14], and studying specific wind turbine blades [15]; the capital cost of the implementation continues to be a frequently studied issue [16].

The development of energy generation systems that use renewable sources have been studied all around the world, including Central America where the rural electrification percentage continues being low [17-22]; there is no literature specifically related to HRES in Costa Rica. But there has been previous research conducted on wind turbines [23], as well as photovoltaic cells and modules efficiency studies [24]. This has allowed Costa Rica to have renewable sources (hydro, solar, wind, geothermal and biomass) that create more than 99% of the energy produced in the country [25].

For this paper, the design was focused in a stand-alone structure, rather than a micro-grid. The system may present problems that should be deeply studied, such as: detachment of the solar panel caused by strong winds that affect the location where they are implemented, insufficient energy production or high energy amounts lost. The study of this new structure design is based on the social problems that are affecting an urban-marginal settlement of 23 hectares in Costa Rica, called Martina Bustos. This territory hosts around 500 families and they are living in insecure housings, but one of the biggest challenges is the lack of electric energy.

Based on all the social and economic issues presented in this specific location, it was considered necessary to study a variety of different projects that can facilitate the quality of life of the inhabitants in the studied community. Therefore, the purpose of this paper is to offer a safe structure that can be resistant to conditions of natural disasters involving the wind's incidence and at the same time, satisfying the electric energy demands in a vastly remote location through wind solar HRES.

2. Materials, methods and calculations

The methodology of the research consists of seven sections. The first and second are associated to energy demand (2.1) and the modeling proposal of the HRES configurations consisting of PV and wind turbine (2.2), respectively. The third section (2.3) defines electricity generation on each configuration presented on (2.2). Further, (2.4) presents a comparison between energy demand and energy generation of the systems. During the fifth section (2.5), the calculation process of the

wind force and overturning moment of the system is estimated. A safety analysis is realized on each of the structures (2.6). In the last section (2.7), the calculations made on the previous steps allow it to state the parameters of effectiveness of systems proposals, on the specific location.

2.1 Energy demand for Government free housing

A Government free housing is a house granted by banks to families or single parents with low economical resources in Costa Rica. Houses have two bedrooms, a living room, a dining room and a kitchen; it counts with thirteen outlets and seven lights in an area of 42 m². For the study of energy consumed, shown in Figure 1, it was necessary to calculate electric bills of four Governmental free housings. Electric bills were collected from the Costa Rican Institute of Electricity. The energy consumption study showed that on average, one house needs a system to produce 7 kWh daily in order to cover the necessities of four habitants.

2.2 Structures configurations

Eighteen structure configurations of wind turbines and solar panels were determined as shown on Table 1. From all the configurations nine possible combinations were designed on ten different models as shown on Figure 2. On which, there are three special structures: III-VI-IX, which are conformed by top panels and bottom panels. In order to be considered a HRES, the system must include solar panels and wind turbines; configurations that do not follow this "rule" should be discarded, in this case combinations 1 and 10.

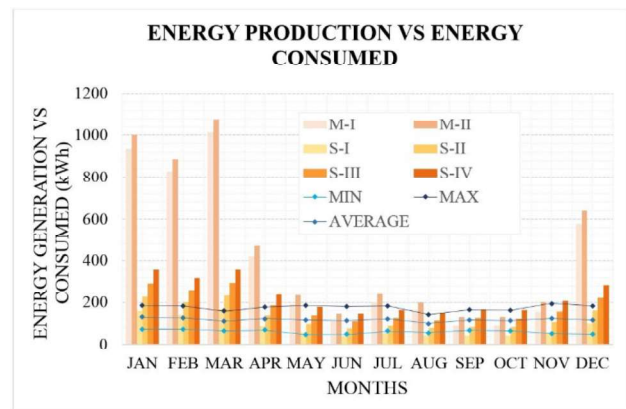


Fig. 1 Energy production (vertical bars) vs energy consumed (horizontal lines)

Table 1 Structure configurations

Combination	Wind turbine	Panel position		Model
		Top	Bottom	
1	Airdolphin	0	0	None
2		0	1	I, VIII
3		0	2	II, V
4		1	0	X
5		1	1	IX
6		1	2	None
7		2	0	IV, VII
8		2	1	VI
9		2	2	III
10	Zephyr 9000	0	0	None
11		0	1	I, VIII
12		0	2	II, V
13		1	0	None
14		1	1	None
15		1	2	None
16		2	0	None
17		2	1	None
18		2	2	None

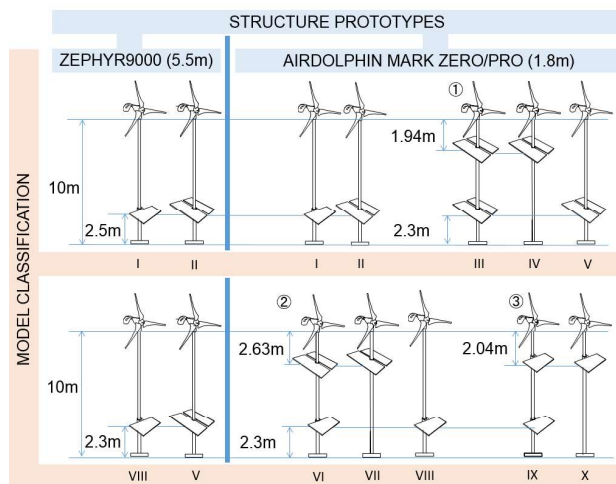


Fig. 2 Structures prototypes and model classification

Wind turbine size affects the model design. In a 10-meter height tower with a medium turbine (Zephyr9000), it is difficult to design more than two vertical solar panels. Therefore, combinations 13 to 18 were not used for the purpose of this paper.

In addition, combination 8 was not considered because two top panels would create a shade on bottom panels that would affect energy production, considering the inclination angle of the solar panel (15) used.

The vibration analysis and its coupling with the performance of the solar panel is beyond the scope of the investigations. But despite of being out of reach, to place the

solar panels in a structure like the one proposed, the effect of the turbine's vibration must be considered; therefore, suitable anti-vibration mounts must be introduced in the eventual construction and assembly of this renewable energy solution.

The position of top panels in special structures was defined by the shading angle. The wider the shading angle, the bigger amount of direct normal irradiation that can be obtained in the bottom solar panel.

The parameters of shading angle on special structures ①②③ were defined differently on each structure. On special structure 1, it was calculated up to 70° with no projected shadow on the bottom panels. On the contrary, on special structure 2 and special structure 3 were up to 80° that will not project shadow on the bottom panel.

2.3 Energy generation

Energy generation of HRES was calculated by adding the amount of energy produced by its two components; the solar panel(s) and the wind turbine. This calculation does not include the amount of energy losses as shown in Figure 1.

2.3.1 Wind resource

The wind speed data at the specific area was collected from the National Meteorological Institute of Costa Rica at Daniel Oduber Quiros International Airport, Basin 74, station 51 (Confidential information). The wind speed in nearby locations can be obtained with statistical models [26]. The data was used to calculate the energy generation of two specific wind turbines; Zephyr9000 and Airdolphin Mark/Zero-Pro with a rotor diameter of 5500 mm and 1800 mm respectively; manufactured by Zephyr Corporation.

Hourly wind speed of a single year was estimated and used to calculate energy generation of wind turbines in the specific location.

Several parameters were utilized to determine the speed data that would not generate enough electricity. Some of the criteria include:

- 1) Hourly wind speed greater or equal to 2.5 m/s in the case of Airdolphin Mark-Zero/ Pro turbine.
- 2) Hourly wind speed greater or equal to 3.0 m/s for Zephyr9000 turbine.

At last, the amount of energy that can be generated, was calculated according to the specific wind speed data [27] by using the following equations (1) and (2):

$$P_{\text{Turbine}} = \text{Efficiency} * P_{\text{wind}} \quad (1)$$

$$P_{\text{wind}} = \frac{1}{2} * \rho * A * v^3 \quad (2)$$

Where $P_{Turbine}$ is the power that can be extracted at a certain wind speed (W), Efficiency = 35% (Standard: 30% ~ 40%), P_{wind} (W) is the available power in the wind (W), ρ is the air density in the specific location (1.225 kg/m^3), v is the wind speed (m/s) and A is the rotor swept area (m^2).

2.3.2 Solar resource

Data of solar irradiation per month was collected from Martina Bustos (Latitude: 10.658838, Longitude: -85.421436) using the software ArcGIS [28].

A base panel from Canadian Solar (330P, 992 cm x 1960 cm) was used to calculate the amount of energy generated by one or more solar panels. These calculations [29] were done, through the use of equations (3) and (4):

$$E = (P * SPH * PR * D)/1000 \quad (3)$$

SPH = Direct normal radiation * k factor (15 degrees - inclination angle). (4)

Where E is the energy in kWh generated each month, P is the power (330 W), $PR = 0.75$ (default value), D is the number of days, and SPH stands for sun peak hours.

2.3.3 Maximum energy production of HRES structures

Energy production of the different HRES systems; was calculated by adding the energy production of the solar panel (equations (3) and (4)), specified on point 2.3.2 and the energy production of the wind turbines (equations (1) and (2)), defined on point 2.3.1.

2.4 Energy production vs Energy consumption

Energy production of each HRES proposed and the energy consumed in a Government free housing, were compared as shown in Figure 2, to select the structures which work more effectively, considering the necessities of the community location.

2.5 Wind force and overturning moment calculation

Calculation of the wind force of the HRES was made in two parts:

Part I: Calculation of the design wind force and overturning moment of wind turbines when the blades are not rotating, by using theoretical calculations.

Part II: Experimental analysis of the pole and solar panel structures performed in a wind tunnel.

2.5.1 Theoretical design

Wind force and moment calculations [30-31] of the wind turbines were made by using the following equations (5) and (6).

$$F = C_f * \frac{1}{2} * \rho * V_{e50}^2 * A_{proj} \quad (5)$$

$$M_b = F * H \quad (6)$$

Where F is the wind force (N), C_f is the wind force coefficient [31], V_{e50} is the design wind speed (m/s), A_{proj} is the projected area perpendicular to the wind direction (m^2), M_b is the moment in the base (Nm) and H is the height of the tower (10 m).

Theoretical calculations of equipment restrictions were made on the turbines where the blades were not moving. These were compared with a commercial wind turbine rotor in movement to define how the turbines may be affected by this limitation, which presented a low error percent.

The successful validation of wind force results was made through thrust force calculations by using WFD500W-B of Suzhou Yueniao Machinery & Electronics Imp. & Exp. Co Ltd. [32], as a reference turbine. This wind turbine has a rotor thrust at 20 (m/s) of 175 (N) and a rotor diameter of 2.0 (m). Equation (5) was used to calculate wind force on the manufacturer company reference data.

These results were used to demonstrate the efficacy of the calculations made on the wind turbines of the HRES configurations tested in this paper. The results confirmed that the value of Wind force of the reference turbine administered by the manufacturer (175 N), is similar to the calculations made (174.45 N) from using equation (5), demonstrating that this equipment limitation in the experiment does not significantly impact the results of the tests configurations.

2.5.2 Experimental analysis

The Eiffel-type boundary layer wind tunnel of the Wind Engineering Research Center at the Tokyo Polytechnic University [33], was used to perform wind force experiments of the solar panel and the pole (Figures 3 and 4).

The wind tunnel length is 33.1 m , with a test section of 19.1 m long. The cross-section of the measurement cylinder (test section) dimensions are 1.8 m height and 2.2 m wide, with a contraction ratio of $\frac{1}{4}$, wind velocity between 0.5 m/s ~ 15 m/s , and average wind speed deviation of $\pm 1.0 \%$. A turbulence grid was used to simulate the wind conditions of Martina Bustos as shown on the Figures 7 and 8. Specific

machinery of wind force measurement was also located in this section.

A. Instrumentation

To obtain the data of the experimental part into the computer, a variety of instruments were used; these instruments are explained bellow.

A Short Probe [1] and an I-Type Probe [2], which are shown on Figure 5, are anemometers that were used to measure the wind speed in the wind tunnel. The I-type probe used in the experimental setup was a Model 0251R-T5 (Japanese company Kanomax Japan. Inc). This anemometer has a resistance of 4.74 Ω at 100 °C, a temperature coefficient (x1/1000) of 3.70, with a recommended operation resistance of 5.38 Ω, and a recommended operation temperature of 150 °C.

A turntable is a circular table that turns depending on the angle. The turntable was formed by six supports [1], a dynamic force balance [2] and an H-shape frame [3], as shown on Figure 6. Turntables were protected with two different covers [1] and a turbulence grid made of wood [2], as shown on Figure 7. Several acquisition equipment were used, as shown on Figure 8; including: an instrument of wind force calibration [1], a strain amplifier [2], a probe amplifier and linearizer [3], and the wind tunnel control panel [4]. The pitot tube was used to measure fluid flow velocity by measuring static and dynamic pressure difference. A monitor of velocity pressure [1] and an AD (analog to digital) converter [2], as shown on Figure 9.

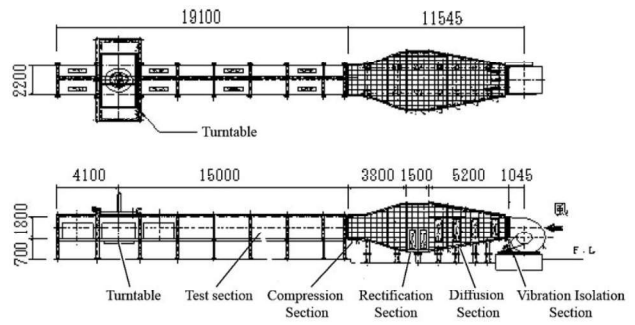


Fig. 4 Wind Tunnel Pattern diagram

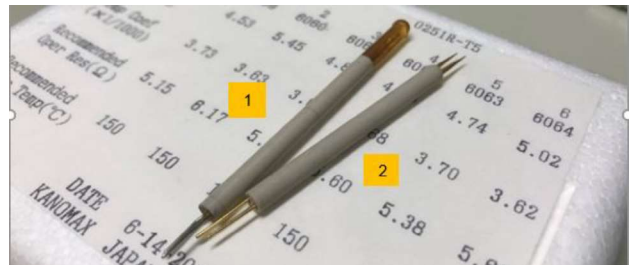


Fig. 5 Anemometers

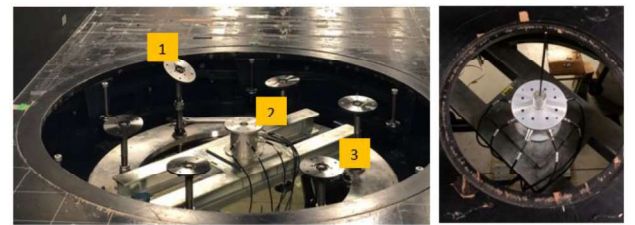


Fig. 6 Turntable



Fig. 3 Wind Tunnel design diagram

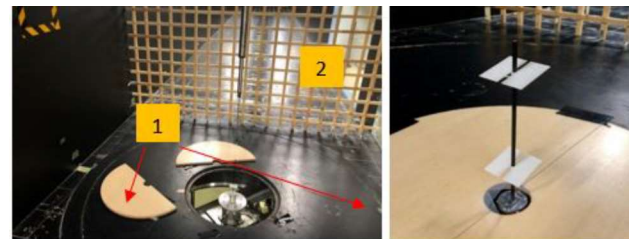


Fig. 7 Covers and turbulence grid

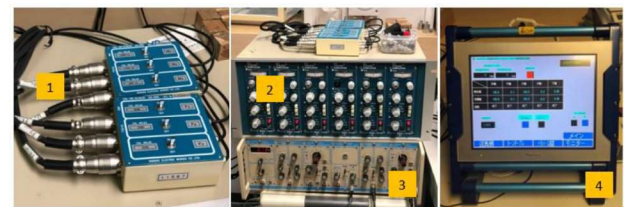


Fig. 8 Acquisition equipment

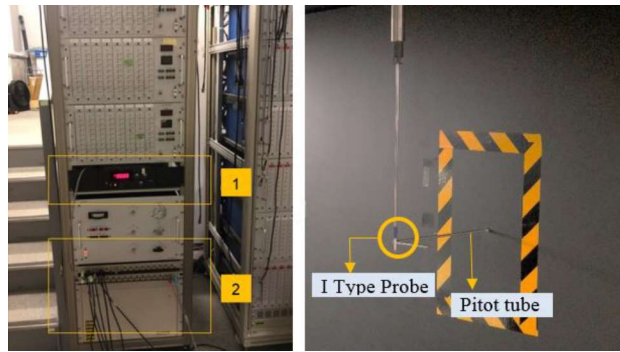


Fig. 9 Instruments of monitoring and measurement of velocity pressure

B. Dynamic similitude

To guarantee the validity of the experimental procedure with scale models, with respect to the expected real results, the dynamic similarity was ensured through the consistency between the Reynolds number of the experimental setup and the Reynolds number obtained in real conditions.

The Reynolds number was calculated by using the equation (7):

$$Re = (V * D)/\nu \quad (7)$$

Where; Re is the Reynolds Number (dimensionless), V is a characteristic flow velocity (m/s), D is a characteristic linear dimension (m), and ν is the kinematic viscosity of the fluid (m^2/s).

The experimental part was finished within an air temperature of 20°C, which possess a kinematic viscosity of $1.51 \times 10^{-5} (m^2/s)$, with specific model length of 0.25 (m) and velocity speed of 10 (m/s). The real measurements were 10 (m) and 10 (m/s) respectively. Based on the experimental and real measures from equation (7), it was not possible to achieve the Reynolds Number (Re) of 2.6×10^7 . This number corresponds to the real conditions as shown in Table 2, at a critical wind speed of 40 m/s. Instead, a $Re = 1.6 \times 10^5$ was selected because the drag coefficient of a cylinder (equivalent to the pole used in the experimental analysis), is similar at both Re and are placed out of the drag crisis region [34-35].

Table 2 Reynold's number specifications

STRUCTURE	EXPERIMENT	REAL
Flow velocity (m/s)	10	40
Linear dimension (m)	0.25	10
Kinematic Viscosity (m^2/s)	1.51×10^{-5}	
Reynolds number	1.6×10^5	2.6×10^7 .

C. Measurements of wind force and overturning moment coefficients.

The models had solar panel(s), each of 5 x 2.5 cm and a tower of 25 x 0.5 cm. Models were mounted on the dynamic force balance shown on Figure 6. Tests were done at constant wind speed of 10 m/s.

Wind force coefficient C_f and overturning moment coefficient C_M of one sample was measured for 60 s. Each sample was measured five times at 300 Hz sampling frequency, with an angle of direction from 0 degrees to 180 degrees with 19 intervals of 10 degrees each, as specified on Figure 10.

Each force was directly measured with the dynamic force balance connected to the wind force calibration instrument and the strain amplifier. An average of the five measurements was used to evaluate the data of C_f and C_M each value with its own definition of direction as shown on Figure 10. These values were calculated with the following equations (8) and (9) [31]:

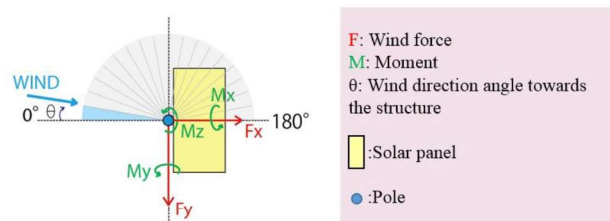
$$C_f = \frac{F}{\frac{1}{2} * \rho * \bar{V}_H^2 * A_{Proj}} \quad (8)$$

$$C_M = \frac{M}{\frac{1}{2} * \rho * \bar{V}_H^2 * A_{Proj} * H} \quad (9)$$

Where; C_f is the wind force coefficient, \bar{V}_H is the mean wind speed (m/s), A_{Proj} is the area of a solar panel = $(B * D)$ with values of $B = 0.05$ m, $D = 0.025$ m and H is the tower height 0.25 m.

Each hybrid wind-solar energy system analyzed on the wind tunnel was re-named with roman letters for better understanding, as shown on Tables 1 and 3. The mean maximum of the ensemble mean of the wind force coefficient was calculated.

The data obtained in the experimental process, was used to determine wind force coefficients of axis X, Y and Z on each system, as shown on Figure 11.



** There is also a F_z not visualized in the figure.

Fig. 10 Definition of wind force and overturning moment direction

Table 3 Structures classification

Structure	Classification	Equivalent combination
Pole + Single panel	I	2,11
Pole + Double panel	II	3,12
Special 1 Whole structure	III	9
Special 1 Top panels	IV	7
Special 1 Bottom panels	V	3,12
Special 2 Whole structure	VI	8
Special 2 Top panels	VII	7
Special 2 Bottom panel	VIII	2,11
Special 3 Whole structure	IX	5
Special 3 Top panel	X	4

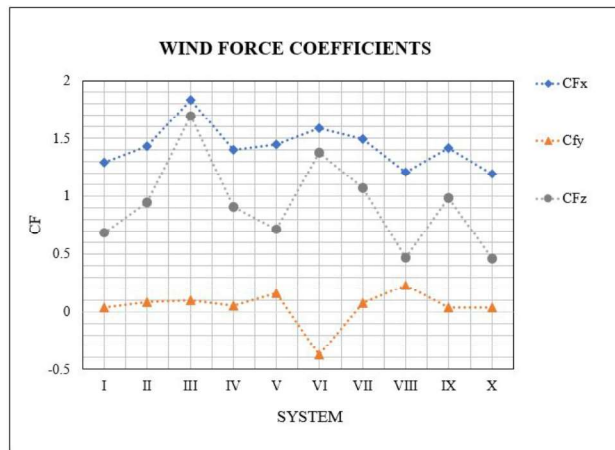


Fig. 12 Overturning moment coefficient (CM)

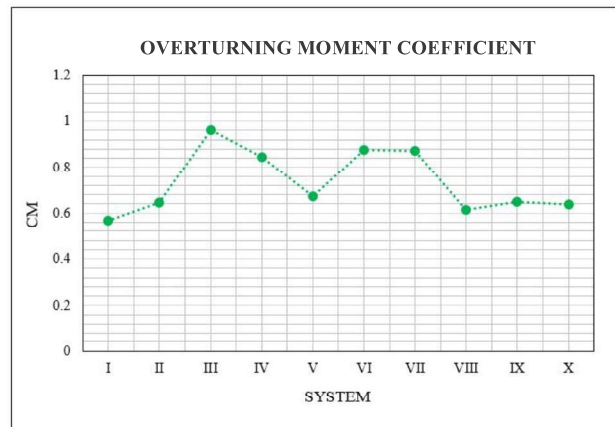


Fig. 11 Wind force coefficients (CFx, CFy, CFz)

The overturning moment coefficient was calculated by applying the vector addition to obtain the resultant of the values of CFx, CFy and CFz, from each degree (0-180). Next, the maximum resultant was selected as overturning moment coefficient on each system, as shown on Figure 12.

D. Calculation of wind force and overturning moment values

After the wind force coefficient and overturning moment coefficient were calculated, they were normalized into the real-size structure measurements using equations (8) and (9), considering the natural resources and conditions of Martina Bustos, analyzed previously.

2.5.3 Wind force and overturning moment coefficient values of the hybrid renewable energy system (HRES)

Wind force and overturning moment of the HRES were based on the summary of each of the sub-systems (wind turbine and solar panel + pole) values calculated through the experimental part and the theoretical calculations data presented on section 2.5.1. for each, the wind force and overturning moment.

2.5.4 Specification of HRES overturning moment values

As shown in Figure 13, when comparing the overturning moment on each pole of the different HRES structures; in all the HRES structures designed, each pole possesses a big change in the overturning moment values because of the utilization of different wind turbines.

The structures which contain the medium wind turbine: Zephyr9000, (M-I, M-II, M-V and M-VIII), present a greater overturning moment on the pole than the structures that contain a small wind turbine (S). The reason of this big change in overturning moments values, is that, the component area projected onto a plane perpendicular to wind direction in a medium wind turbine, is greater than a small wind turbine.

Therefore, while comparing S-III, which is the HRES structure that utilizes the larger number of solar panels, the overturning moment is similar to the system that uses the big wind turbine.

On a similar note, when analyzing the system safety during the utilization of the overturning moment calculation of the HRES on the next point 2.6, the results show that the medium sized wind turbines have an overturning moment value with greater steel plate thickness, compared with the other HRES structures as shown on Table 4.

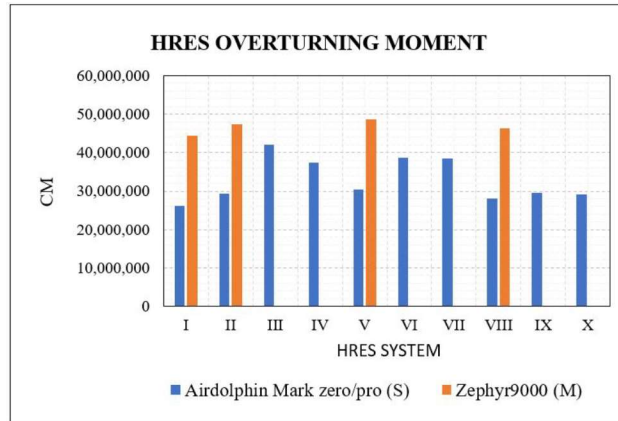


Fig. 13 HRES overturning moment values

2.6 System Resistance to strong winds

Overturning moment was analyzed to define the system safety to local buckling through load allowable stress calculations [36] of the HRES, with the objective to find the adequate tower thickness. Steel SS400 was used as the tower material since it is one of the most commonly used hot rolled general structural steel materials used in Japan, because of its low price, excellency in weldability and machinability. This material is supplied as plates, flats, bars and others [37]. The used equations follow:

$$\sigma = \frac{M}{Z} \leq f_b \tag{10}$$

Where; $Z = \frac{I}{D/2}$ (11)

$$I = \frac{\pi \cdot D^4}{64} - \frac{\pi \cdot d^4}{64} \tag{12}$$

$$\sqrt[4]{D^4 + \frac{32 \cdot D \cdot M}{\pi \cdot f \cdot b}} \geq d \tag{13}$$

$$t = \frac{D-d}{2} \tag{14}$$

Where; σ is the load allowable stress (N/mm^2), f_b is the allowable bending stress of the material, I is the moment of inertia (mm^4), Z is the section modulus (mm^3), D is the diameter of the tower/pole (mm), t is the steel plate thickness (mm), d is the interior diameter (mm) and M is the vector sum of M_x and M_y , defined as the overturning moment.

In a diameter of 200 mm, the thickness of the steel plate was calculated, according to JIS G 3101-1998 [36]; as shown on Table 4.

The influence of the DTR (diameter - thickness ratio) [36] on the stability and response of circular structures, in this case, the tower (pole), was necessary to define the safety of the system. This was calculated with equation (15).

$$DTR = D/t \tag{15}$$

DTR was defined as $(D/t \leq 70)$, where; any of the designed systems can resist strong winds and be safe of local buckling.

2.7 Selection of the suitable HRES structure

The correlation of tower thickness, turbine size, number of panels and energy generation of each of the proposed models are summarized in figure 14. This correlation simplifies the process of the adequate structure selection.

Figure 14 shows that there are ten classified systems per wind turbine. As explained in point 2.3 structure configurations, six system classifications do not apply for medium wind turbines. All of the systems are safe to local buckling ($D/t \leq 70$) as specified in point 2.6.

3. Discussion

All proposed HRES structures generate the greatest amount of energy during the first months of the year, with a peak between December and January as shown on Figure 1. There is a decrease from April to October. However, each turbine has a different cut-in wind speed value; therefore, the structures composed by the wind turbine of the biggest size, Zephyr9000, with a cut-in of 3 m/s have an extreme change on the energy generation during March-June. Consequently, the energy generation during some months, is lower than the energy required. On the other hand, it is easy to denote in the same figure, that a small wind turbine with four panels, is able to generate more electric energy than a big turbine, during the months with lower wind speeds. This is because the cut in wind speed is 2.5 m/s. Since this analysis was made according to wind speed data of 10 years, it is not expected to present a variation in the near future.

Table 4 Definition of t value (mm)

Structure	Wind turbine (S)	
	t value Calculated	t value (JIS)
I	3	4.5
II	4	4.5
III	4	4.5
IV	6	6
V	6	6
VI	4	4.5
VII	6	6
VIII	4	4.5
IX	4	4.5
X	4	4.5

Zephyr9000, the calculated thickness value was 7 mm and the thickness value according to JIS was 8 mm in all the structures.

Wind turbines of great magnitude, in a tower with a height of 10 meters, cannot be designed as special structures (structures that possess top and bottom panels) because of the high wind speeds generated by the rotation of the blades. However, small wind turbines can be used on special structures when specific panel position calculations are made adequately. Under these circumstances, and they can generate the desirable amount of energy in the precise location.

The values of overturning moment studied on Figure 12 and wind force calculated through experiments on Figure 11, show that the special structure 2- whole structure (III), possess the greater values. Coefficients of wind force on the axis X and Y of the different structures as shown on Figure 11, demonstrated that the larger the projected area of the structure is, the bigger the value of the coefficient becomes, as expected.

Overturning moment values are calculated with the projected area and the height of the tower, as well as the height related to the position of the panels, as shown on Figure 12.

On diameter to thickness calculations, it is essential to understand that the smaller the DTR is, the higher the resistance to local buckling becomes.

This local buckling occurs similarly to the one of a steel pipe, inside the cavity of the pillar. If the measure of the plate thickness becomes larger, the structure turns out to be more resistant to local buckling.

The results of these calculations shown on Table 4, are defined according to JIS in a steel plate thickness greater than the calculated, for this reason each tower could be considered more resistant to strong winds if this value is taken.

Costa Rica has the potential to implement this kind of structure in different zones of the country. The use of a design wind speed of 38.8 m/s, assigned to the area of Martina Bustos, were utilized to calculate the wind force and overturning moment values on the proposed models. These were used to calculate allowable stress design on the tower of 10 m height, to determine the resistance to local buckling. All the results were positive.

Four of ten structures can produce the energy needed all year-long in Martina Bustos and all of these structures can withstand wind forces that may produce local buckling on the tower as presented in Figure 12. On each structure a satisfactory calculation of steel plate thickness was made, which leads to different HRES thickness. The values found were: 4.5 mm, 6 mm or 8 mm.

According to Figure.14, there are four structures (S-III, S-VI, M-II, M-V) that cover the average electric energy consumed in a government free housing for twelve months. Based on this data, the summary chart and the energy production vs energy consumed graphic of the Figure.1, system S-III covers the energy consumption of twelve months of the year as does the S-VI structure. However, because of the number of panels it produces more energy than the S-VI for the entire year, and even more than systems M-II and M-V consume in four months.

When analyzing the results presented in Figure 14, it is worth noting that none of the three proposed structures with a single panel are capable of satisfying the demand for more than 3 months, with a small wind turbine; nor for more than 9 months in the case of the large turbine. With this result, HRES with a single solar panel could be discarded. Furthermore, if the structure is composed only by one panel and presents a failure, the use of the solar resource would be totally lost.











HYBRID RENEWABLE ENERGY SYSTEM										
Specifications	Summary of data									
	I	II	III	IV	V	VI	VII	VIII	IX	X
										
AIRDOLPHIN (S)										
Thickness	t= 4.5	t= 4.5	t= 4.5	t= 6	t= 6	t= 4.5	t= 6	t= 4.5	t= 4.5	t= 4.5
Number of months when: Coverage > Average Consumed	3	5	12	5	5	12	5	3	5	3
ZEPHYR9000 (M)										
Thickness	t= 8	t= 8	Does not apply		t= 8	Does not apply		t= 8	Does not apply	
Number of months when: Coverage > Average Consumed	9	12			12			9		
All of the structures presented in this chart, possess a Diameter to thickness ratio (DTR) ≤ 70										

Fig. 14 Summary chart

The difference in these three systems is not only the number of panels and energy generation, but also the size of the wind turbine used. Between systems M-II and M-V, the only difference would be the position of the solar panels specified on Figure 2. Models S-II and S-V have the same position of the solar panel but have a different turbine size causing changes in thickness values which can affect the price of the system. This makes the S-V the most expensive energy source.

Systems M-II and M-V have wind turbines with bigger rotor radius than systems S-III and S-VI. The implementation of big turbines in the specific location, may impact the environment by causing negative effects on the passage of migratory birds that fly through the area every year. Towers may also produce vibration causing the turbines to generate noise, which may have an effect on the houses near the tower. Therefore, it is recommended for this area, specifically, to implement the construction of a system that contains small wind turbines (S-III or S-VI) rather than larger ones (M-II and M-V).

Based on this analysis the structure that best suits the goals, is the HRES S-III because it has the same tower plate thickness as S-VI and same energy generation. As a consequence, these systems present the same cost in tower construction but different in solar panel implementation. For this reason, the initial cost of the system can be effectively lower in structure S-VI.

But considering unexpected failures that the structure may present, if one of the solar panels stops working, there would be only two panels generating electricity on HRES, which contain small wind turbines. However, two solar panels would not be able to produce more than the average required energy for a year. For this reason, by analyzing these results, the most suitable HRES for a long-term energy production is the HRES S-III, even though the initial cost may be higher than S-IV. This structure also supplies more than the energy consumed in a house that allows one house to share electricity with another.

From a technical worldview, considering the analysis of energy generation and consumption described in points 2.3 and 2.1, calculations of wind force and overturning moment, explained by our experimental processes and theoretical design methods in point 2.5, and lastly, the analysis of safety designs considering the overturning moment values on each pole in point 2.6, it can be concluded that structure S-III is the most effectively adequate for the present concern of this project. The S-III structure specifically satisfies the electrical demand for one full year, and importantly fulfills the Japanese Industrial Standards that take into account the influence of shading effects on the structures, as well as security and safety measures when climatological data of the location used, is in effect.

This analysis of results for this study case can be extended to other cases where the consumption data and the characteristics of the turbines and panels are available, thus giving more value to the paper for its applicability to HRES in remote areas. This is the first study that considers HRES in Costa Rica. It uses real data of energy production and consumption while combining the structure security meticulously; without neglecting the specific geographic location with real wind velocity data and solar irradiation, providing valuable design guide for further research.

4. Conclusions

In this paper, HRES (solar-wind) configurations were designed according to a specific location parameter in Costa Rica, based in Japanese Industrial Standards. Systems were designed and tested to supply electric energy to government free housings in a remote location, Martina Bustos; through analytic and experimental process while testing in a wind tunnel.

The found conclusions follow:

- HRES are a viable solution to the energy problem in developmental countries where houses present a low energy consumption.
- For remote areas it is more convenient to install a wind turbine with a low cut-in wind speed, because the Eolic potential is low, so that, a 0.5 m/s lower represents a great impact on the energy production.
- For the HRES system, the most convenient turbines are the small ones because they allow the implementation of more solar panels and they can also be configured so the residual does not affect them.
- It is not recommended for HRES to use a single solar panel, in structures with a small wind turbine. This may affect the power output of the system.
- The structure S-III, conformed by four solar panels (two top panels and two bottom panels), is the most suitable for Martina Bustos. The use of small wind turbines produces less impact on the environment.

These innovative solutions needed, to supply electric energy to remote areas; particularly requires, the participation and empowerment of the local inhabitants. The maintenance of HRES is essential to guarantee a longer lifespan and the use of remote off grid systems provides a truly sustainable solution in a long-term to the energy concerns in Martina Bustos.

Acknowledgements

This work had enjoyed full funding on model's fabrication and technical assistance from the Tokyo Polytechnic University where the laboratory experiments were carried out.

The first author gives a sincere and special gratitude to the Meteorological Institute of Costa Rica, to the research laboratories of the Costa Rica Institute of Technology: LIENE and SESLab and to Prof. Yong Chul Kim and Prof. Akihito Yoshida of the Tokyo Polytechnic University, who supported this research.

References

- [1] IEA/OECD (2018), World Energy Outlook. International Energy Agency, France.
- [2] REN21. (2018). Renewable Global Status Report Renewable Energy Policy Network for the 21st Century.
- [3] D.A. Lashof, & D.R. Ahuja. (1990) "Relative contributions of greenhouse gas emissions to global warming". Nature.
- [4] BBC. (2019). Energy demands and resources. BBC.
- [5] S. Kotra, & M. K. Mishra. (2015) "Energy management of Hybrid Microgrid with Hybrid energy Storage System" 4th International Conference on renewable Energy Research and Applications (ICRERA). vol. 5, pp. 856-860. Palermo, Italy.
- [6] Y. Yang (2014). "An analysis of hybrid energy system: A case study". Morehead State University. Theses and Dissertations. 63. pp 8-19.
- [7] Y. W. Kean, A. Ramasamy, S. Sukumar, & M. Marsadek. (2019) "Adaptive Controllers for Enhancement of Stand-Alone Hybrid System Performance". International Journal of Power Electronics and Drive System (IJPEDS), vol. 9, no. 3, pp. 979-986.
- [8] B. Madaci, R. Chenni, E. Kurt, & K. E. Hemsas. (2016) "Design and control of a stand-alone hybrid power system" International Journal of Hydrogen Energy, vol. 41, no. 29, pp. 12485-12496.
- [9] A. Vargas-Martínez, Y.M. Zhang, & L. E. Garza-Castañón, E. R. Calle Ortiz and J. César Viola, (2013) "Model-based control approaches for optimal integration of a hybrid wind-diesel power system in a microgrid" 2nd International Conference on Smart Grids and Green IT Systems. Pp 12-21. Aachen, Germany.
- [10] E. H. Enrique, S. Moser, & T.P. Bailey. (2017). "Capacitor banks contribution to Arc-flash. Applications to solar and wind farm substations". 6th International Conference on Renewable Energy Research and Applications. pp. 389-394. San Diego, CA, USA.
- [11] L. Ramirez Camargo, K. Gruber, F. Nitsch, & W. Dorner. (2018) "Hybrid renewable energy systems to supply electricity self-sufficient residential buildings in Central Europe". 10th International Conference on Applied Energy (ICAE2018). Energy Procedia, vol. 158, pp. 321-326. Hong Kong, China.
- [12] I. Padrón, D. Avila, G. N. Marichal, & J. A. Rodríguez. (2019). "Assessment of Hybrid Renewable Energy Systems to supplied energy to Autonomous Desalination Systems in two islands of the Canary Archipelago". Elsevier BV. Renewable and Sustainable Energy Reviews, vol. 101, pp. 221-230. Spain.
- [13] A. Razmjoo, R. Shirmohammadi, A. Davarpanah, F. Pourfayaz, & A. Aslani. (2019). "Stand-alone hybrid energy systems for remote area power generation". Energy reports. Vol. 5, pp. 231-241. Tehran Iran.
- [14] A. Harrouz, I. Colak, & K. Kayisli. (2016). "Control of a Small Wind Turbine System Application". 5th International Conference on Renewable Energy Research and applications (ICRERA). pp. 1128-1133. Birmingham, UK.
- [15] J.S Bae, D. G Choi, S. Y Lee, C. Yoo, & D. J. Kim. (2015). "Preliminary Study on Fabric-Covered Wind Turbine Blade". 4th International Conference on Renewable Energy Research and Applications (ICRERA). pp. 1196-1200. Palermo, Italy.
- [16] R. Goddard, L. Zhang, & X. Xia. (2018). "Optimal Sizing and Power Sharing of Distributed Hybrid Renewable Energy Systems Considering Socio-Demographic Factors". South Africa. Applied Energy Symposium and Forum, Renewable Energy Integration with Mini/Microgrids, REM 2018. Energy Procedia, vol 159, pp 340-345. Rhodes, Greece.
- [17] R. Madriz-Vargas, A. Bruce, M. Watt, L.G. Mogollón, & H.R. Álvarez, (2017) "Community Renewable Energy in Panama: a sustainability assessment of the Boca de Lura PV-Wind Hybrid Power System", World Renewable Energy Congress XVI. Western Australia.
- [18] D. Ley. (2013). "Sustainable Development, Climate Change, and Renewable Energy in Rural Central America." Oxford University, United Kingdom.
- [19] R. Madriz-Vargas, A. Bruce, M. Watt, (2017). "Community Renewable Energy in Nicaragua: Sustainability Assessment of APRODELBO", National University of Costa Rica.
- [20] R. Madriz-Vargas, A. Bruce, & M. Watt (2017). "A cross-case Analysis of needs and opportunities from Community Renewable Energy Projects in Central America" Asia-Pacific Solar Research Conference. Melbourne, Australia.
- [21] R. Madriz-Vargas, A. Bruce, & M. Watt, (2018) "The future of Community Renewable Energy for electricity access in rural Central America", Energy Research and Social Science, vol. 35, pp. 118-131.

- [22] G. Richmond-Navarro, R. Madriz-Vargas, N. Ureña-Sandí, & F. Barrientos-Johansson. (2019). "Research Opportunities for Renewable Energy Electrification in Remote Areas of Costa Rica". *Perspectives on Global Development and Technology*, Vol. 18. No. 5-6. pp.553-563.
- [23] G. Richmond-Navarro, G. Murillo-Zumbado, P. Casanova-Treto, & J.F. Piedra-Segura. (2019). "Estado actual de la investigación sobre turbinas eólicas en Costa Rica". *Revista Tecnología En Marcha*, vol. 32. No. 2. pp.54-67.
- [24] L.D. Murillo-Soto, & C. Meza. (2018) "A Simple Temperature and Irradiance-Dependent Expression for the Efficiency of Photovoltaic Cells and Modules". 2018 IEEE 38th Central America and Panama Convention (CONCAPAN XXXVIII). pp. 1-6.
- [25] T. Embury. (2017). *Costa Rica's electricity generated by renewable energy for 300 days in 2017*. Independent. London, United Kingdom.
- [26] S. Basile, R. Burlon & F. Morales. (2015). "Joint probability Distribution for Wind Speed and Direction. A case of study in Sicily". 4th International Conference on Renewable Energy Research and Applications. pp. 1591-1596. Palermo, Italy.
- [27] J. Jamii, D. Abbes, & M. F. Mimouni. (2019). "Energy Management of Wind Power Generation with Pumped Hydro Energy Storage and Participation in Frequency Control: Study in Electricity Market" *International Journal of Renewable Energy Research*, vol.9, no.4, pp.2082-2091. Tunisia.
- [28] NASA Langley Research Center (LaRC). (2018) *POWER Data Access Viewer*. NASA.
- [29] W. Mora Iturbe. (2018) "Programa administrador de la energía. Especialidad en energía solar para la generación eléctrica eficiente." Complejo Forza Vital, Costa Rica.
- [30] Japanese Standards Association. (2017) "JIS C 8955 (JEMA) Load design guide on structures for photovoltaic array". Pp. 10. Tokyo, Japan
- [31] Japanese Industrial Standards Committee. (2010) "JIS C 1400-2(JEMA) Wind turbines- Part 2: Design requirements for small wind turbines" Japanese standards association. pp 30-71. Tokyo, Japan
- [32] Suzhou Yueniao Machinery & Electronics Imp & Exp Co Ltd. (2010). "Wind Generator WFD500W". China.
- [33] Tokyo Polytechnic University. (2018) GCOE Program. *New Frontie of Education and Research in Wind Engineering*. 'Large turbulent boundary layer Wind Tunnel'. Kanagawa, Japan.
- [34] W. Gao, D. Nelias, Y. Lyu., & N. Boisson. (2018). "Numerical investigations on drag coefficient of circular cylinder with two free ends in roller bearings". *Tribology International*, vol. 123, pp. 43-49.
- [35] B.R. Munson, D.F. Young, & T.H. Okiishi. (2006). "Fundamentals of Fluid Mechanics". 5th edition, John Wiley & Sons, p. 526.
- [36] Architectural Institute of Japan (2005) "Design Standard for Steel Structures - Based on Allowable Stress Concept", pp. 145-169. Tokyo, Japan
- [37] MEADinfo. (2010) "SS400 Structural Steel - An Overview" MEADinfo - Mechanical Engineer's Information Hub.